Modelling the ultraviolet/submillimeter spectral energy distributions of normal galaxies

Cristina C. Popescu & Richard J. Tuffs

Max Planck Institut für Kernphysik, Astrophysics Dept., 69117 Heidelberg
email:Cristina.Popescu@mpi-hd.mpg.de; Richard.Tuffs@mpi-hd.mpg.de

Abstract. We give an overview of the factors shaping the ultraviolet (UV)/optical - far-infrared (FIR)/submillimeter (submm) spectral energy distributions (SEDs) of normal (non-starburst) galaxies. Particular emphasis is placed on the influence of the geometry of dust and stars on the propagation of light through the interstellar medium. Although strong constraints can be placed on the amount and large scale distribution of dust in disks from the appearance of the galaxies in the optical/UV range, this dust does not account for the observed amplitude and colour of the FIR/submm radiation. Additional, optically thick components of dust associated with the young stellar population on large and small scales are required to account for the complete UV/optical - FIR/submm SEDs. Self-consistent models for the calculation of SEDs of spiral galaxies are reviewed, and their predictions for the dust emission and the attenuation of starlight are compared and contrasted.

1. INTRODUCTION

Historically, almost all our information about the current and past star-formation properties of normal galaxies has been based upon spatially integrated measurements in the ultraviolet (UV), visible and near-infrared (NIR) spectral regimes. However, star-forming galaxies contain dust which absorbs some fraction of the emitted starlight, re-radiating it predominantly in the far-infrared (FIR)/sub-millimeter (submm) range.

In view of this, the measurement of current and past star-formation in galaxies - and indeed of the universe as a whole - requires a quantitative understanding of the role different stellar populations play in powering the FIR/submm emission. For this both optical and FIR/submm data need to be used, as they contain complementary information about the distribution of stars and dust. The problem is very complex. Images of galaxies taken in the stellar light and dust emission show that galaxies are very inhomogeneous systems, presenting both small scale and diffuse components, both in the UV and in the FIR. For instance small scale structures show that part of the stellar light can be locally absorbed and re-radiated in the FIR. The diffuse emission shows that another part of the stellar photons can travel some distance in the disk before being scattered or absorbed. In order to quantitatively model these processes one needs to make a self-consistent calculation of the transport of radiation and its re-emission in galaxy disks. The challenge is to identify a model which is sufficiently simple to make the problem tractable, but which can still predict the essential elements of observed SEDs and morphologies. Here we review progress made towards identifying such models for normal galaxies. Models for predicting SEDs for starburst galaxies are considered in the review of Dopita [15].

CP761, *The Spectral Energy Distributions of Gas-Rich Galaxies: Confronting Models with Data*
edited by C.C. Popescu and R.J. Tuffs

2. WHAT SHAPES THE SEDS OF GALAXIES?

There are two fundamental factors to be considered here:

- the intrinsic emission spectrum produced by all stellar populations in a galaxy
- the propagation of photons through the ISM.

The intrinsic spectrum depends on the star formation history and the metallicity evolution of a galaxy. We will not expand on this here since this is covered by the review talk of Leitherer [34]. The propagation of photons through the ISM depend on:

- the amount of dust and its distribution with respect to the stars
- the optical properties of grains
- the amount of neutral gas and its distribution with respect to the young stars

The neutral gas affects the line emission component of SEDs; this topic is covered in detail in the talk of Kewley et al. [27]. The optical properties of grains, which mean their absorption and scattering properties throughout the UV-submm range, depend on the composition and size distribution of the grains. This topic is covered in detail by the review talk of Dwek [17] (see also the talks by Li [33] and by Gordon [23]), and is only briefly touched upon here, in Sect. 4. The amount of dust and its distribution with respect to the stars has received little attention until recently, even though the distribution of dust is the single most important factor affecting the propagation of photons in galaxies. To illustrate this statement one only has to recall that a fixed amount of dust distributed on a scale of a few parsec around stars will have the same effect as 1000 times more dust distributed on kpc scales in the disk. Therefore this review will mainly focus on the effect of the relative geometries of stars and dust on the SEDs. Previous reviews related to this topic include: Calzetti [9], [10], Popescu & Tuffs [44], Kylafis & Misiriotis [30].

We will start with very simple geometries and increase the complexity until we have identify a minimum degree of complexity that can account for observed broad-band UV/optical/FIR/submm SEDs. We will also consider the effect of these models on the UV/optical/FIR/submm surface brightness distributions. In terms of the dust emission, we will place most emphasis on the FIR emission, rather than, for example, on the MIR emission. This is firstly because most of the energy absorbed by grains is re-radiated in the FIR, and secondly, because the FIR colours of a galaxy depend on the strength of the radiation fields in a galaxy, and therefore more directly constrain the propagation of photons in the disk.

Our entry point is to consider geometries with cylindrical symmetry, which are essential for the description of disk galaxies. Spherical symmetry is a more reasonable approximation for the description of dwarf galaxies (e.g. Galliano et al. [22]) and starburst galaxies (e.g. Witt et al. [56], Gordon et al. [24]). The simplest model is the infinite slab/sandwich. A sandwich model, not incorporating scattering, was used by Disney et al. [13] to investigate the attenuation-inclination behaviour of spiral galaxies. This work first emphasised the strong effect of the relative scaleheights of stars and dust on the attenuation. Another version of the sandwich model, this time including scattering, was used to calculate the energy balance between the emission and re-emission of light in the pioneering work of Xu & Buat [61]. In the Xu & Buat formulation there is only one free parameter, the face-on optical depth, which is adequate to account for the energy balance. Apart from its application to the integrated emission from galaxies (Buat & Xu [4], Xu et al. [63]), this particular model was used by Xu & Helou [62] in the modelling of the large-scale dust heating and cooling in the diffuse medium of M 31. A common drawback, though, of models involving infinite slab/sandwich geometries is that they cannot predict the shape of the observed FIR/submm SEDs. Understanding the FIR colours is not only a matter of academic concern, but also provides a further dimension to the predictive power of models, since the FIR colours directly probe the strength of the radiation fields, and, as we shall see, strongly depend on physical quantities of interest, such as SFRs.

In order to also fit the FIR colours, one needs to consider more realistic geometries, where by realistic we mean incorporation of finite disks, bulges and small scale structures:

- finite disks: stars and/or dust
- bulges: stars only
- small scale structures: stars and/or dust

Finite disks are usually described by double exponentials in both radial and vertical direction. Bulges can be described by a variety of forms: de Vaucouleurs, truncated Hubble, spherical with King profile/exponential. We note here that the exact choice of bulge geometry has little effect on the shape of the globally integrated SED, provided that the bulk of the luminosity of the bulge is emitted within an area much smaller than the disk. Small scale structures have been described as small scale dust clouds/clumps (depending on terminology) which, according to the model, may or may not be physically associated with young stars. As we shall see, this different treatment has strong consequences on the prediction of the FIR colours. All or combinations of these geometrical components have been employed by the models introduced in the following papers: Kylafis & Bahcall [29], Bianchi et al. [8], Bianchi et al. [6], Xilouris et al. [58], Silva et al. [50], Granato et al. [25], Kuchinski et al. [28], Popescu et al. [46], Matthews & Wood [35]. All these models were used to account for the optical SEDs, but only three of them (Bianchi et al. [6], Silva et al. [50], Popescu et al. [46]) were used as the basis for a self-consistent calculation of both the stellar and dust emission SEDs. Recently, self-consistent calculations of attenuation and re-emission by dust grains in galaxies have also been done in the work reported by Baes et al. [3] in this volume, and have started to be incorporated in population synthesis models, such as those of Piovan et al. [43] and Rocca-Volmerange [48], also as reported in this volume.

3. MODELS WHICH ACCOUNT FOR THE OPTICAL APPEARANCE OF GALAXIES

The challenge of models which account for optical SEDs is to identify an intrinsic distribution of stars and dust which is consistent with the observed integrated SEDs and surface brightness distributions. To assess whether a particular choice for the geometry of stars and dust is consistent with observations, calculations of the transfer of radiation

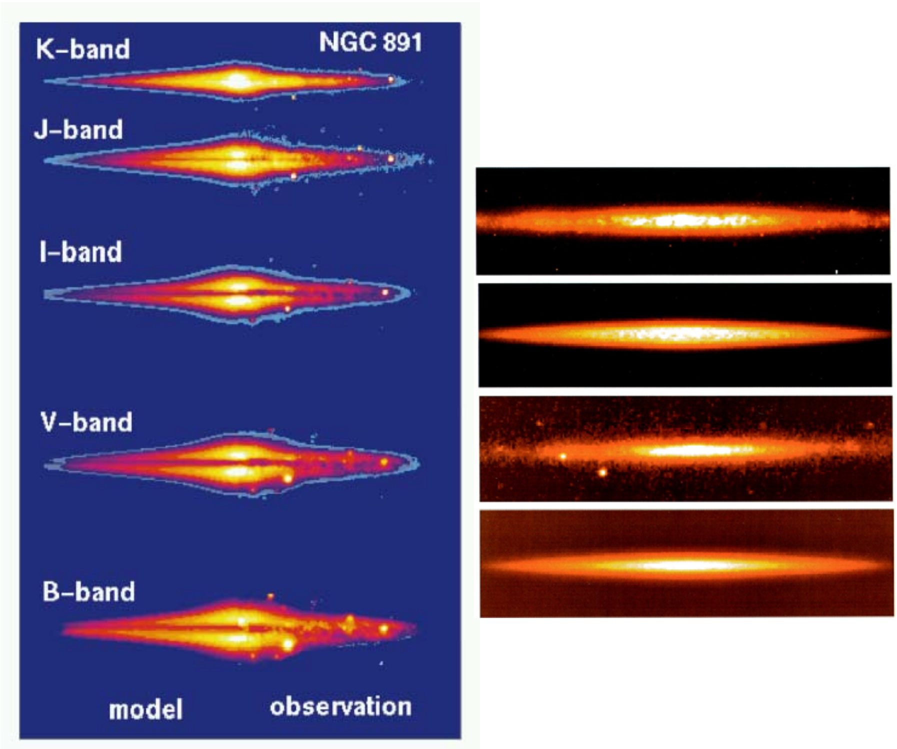

FIGURE 1. Left panel: Images of NGC 891 in K, J, I, V, B bands (top to bottom) taken from Xilouris et al. [59]. The left hand half of each galaxy image is the model image and the right half is the real galaxy image (folded). Right panel: Comparison of R- and H-band Monte Carlo model images of UGC 7321 (second and bottom rows) with real data at these wave bands (top and third row), taken from Matthews & Wood [35].

through the galaxy must be done. Thus, models must incorporate a radiative transfer code. Different radiation transfer codes have been discussed in the review talk of Kylafis & Xilouris [31].

The model of Xilouris et al. [58] derived the relative distribution of stars and dust by fitting optical/NIR images of galaxies, assuming the simplest, yet realistic, distributions of stars and dust that could be used to describe such systems (i.e., exponential disks plus a de Vaucouleurs bulge; see Fig. 1, left panel). This work was done for edge-on galaxies, which allows not only the scalelength but also the scaleheights of dust and stars to be extracted. We should also mention that, since opacities were independently derived at each wavelength, the extinction law was extracted for each modelled galaxy, giving some constraints on the dust model. Apart from the detailed knowledge of the distributions of stars and dust in individual galaxies, some general trends became evident (Xilouris et al. [60]), namely: all the galaxies modeled were able to reproduce Milky Way extinction laws; the optically emitting stars have a scaleheight which is about twice that of the dust;

the dust scalelength is about 1.4 times larger than that of the stars and the dust is more radially extended than the stars. This inference about the relative radial extent of stars and dust can in principle be tested through FIR observations of the dust emission from the regions beyond the stellar disk. This has been done in the case on NGC 891 (Popescu & Tuffs [45]; see also Fig. 2 from the review of Tuffs & Popescu [52]).

Synthetic images have also been compared with observed images by Matthews & Wood [35] (see Fig. 1, right panel), but in this work the geometry was fixed and only the face-on optical depth was varied.

4. MODELS WHICH ACCOUNT FOR THE ENTIRE OPTICAL/FIR/SUBMM SEDS

The challenge of models which account for the entire optical/FIR/submm SEDs is to identify an intrinsic distribution of stars and dust which is consistent with the observed integrated SEDs and surface brightness distributions, both in the optical and FIR/submm ranges. In addition to the radiative transfer code, such models should also incorporate a technique to calculate the dust emission, as outlined below:

For a given spatial distribution of stars and dust, we can calculate the energy densities u_λ at each position in the galaxy through a radiative transfer calculation, which needs to take into account both absorption and scattering. Then, for a given grain model (which in this context means a given grain absorption/emission efficiency Q_{abs}) and a given distribution $N(a)$ in (spherical) grain size a, the energy balance between emission and absorption is given in terms of a probability distribution $P(a,T)$ in the temperature T of each grain by the following equation:

$$\int_0^\infty Q_{abs}(\lambda,a)\,u_\lambda\,d\lambda = \frac{4\pi}{c}\int_0^\infty Q_{abs}(\lambda,a)\,d\lambda\int_0^\infty B_\lambda(T)\,P(a,T)\,\mathrm{d}T$$

Having solved for $P(a,T)$ (see for example Guhathakurta & Draine [26]), the dust emission F_λ can be calculated at each position in a galaxy at distance d using:

$$F_\lambda \quad = \quad \frac{1}{d^2}\int_{a_{\rm min}}^{a_{\rm max}} N(a)\,\mathrm{d}a\,\pi a^2\,Q_{\rm abs}(\lambda,a)\int_0^\infty B_\lambda(T)\,P(a,T)\,\mathrm{d}T$$

where a_{min} and a_{max} are the minimum and maximum grain sizes present in the distribution.

A probability distribution of temperatures arises because grains are impulsively heated by photons. Only when the typical interval between photon hits is much shorter than the timescale for the energy deposited in each photon hit to be radiated does the probability distribution tend towards a delta function - the case of grains emitting at their equilibrium temperature. In general grains smaller than a certain critical size (depending on the strength and colour of the radiation field and composition of the grain) emit stochastically, and grains bigger than this critical size emit at equilibrium temperature. As the radiation fields are increased, grains of progressively smaller sizes radiate

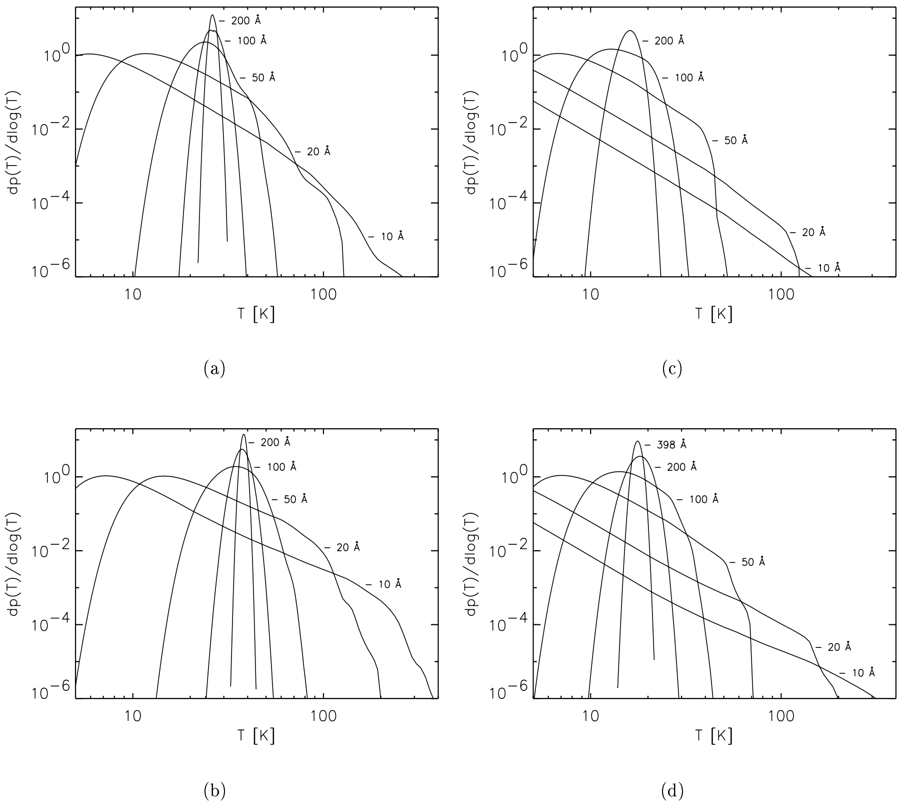

FIGURE 2. Examples of temperature distribution for spherical dust grains (with radii 10, 20, 50, 100, 200, & 398 Å) embedded in the diffuse radiation field of NGC 891, taken from Popescu et al. [46]: a) silicate grains in the centre of the galaxy ($R = 0\,\mathrm{kpc}$, $z = 0\,\mathrm{kpc}$); b) graphite grains in the centre of the galaxy; c) silicate grains at the edge of the galactic disk ($R = 15\,\mathrm{kpc}$, $z = 0\,\mathrm{kpc}$); d) graphite grains at the edge of the galactic disk.

at equilibrium temperature. Conversely, as radiation fields are decreased, grains of progressively larger sizes will radiate stochastically. These trends are illustrated in Fig. 2.

4.1 Choice of intrinsic distributions of stars and dust

The old stellar disk and associated dust

The obvious starting point in identifying a spatial distribution of stars and dust that can account for the entire optical/FIR/submm SED is to test whether the distributions which are consistent with the observed optical SEDs can also account for the FIR/submm

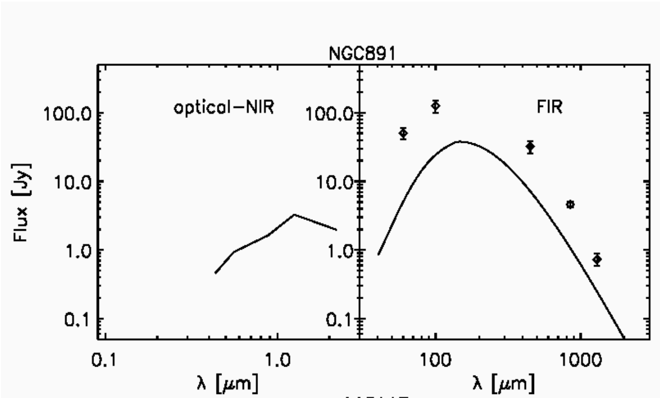

FIGURE 3. The FIR/submm SED of NGC 891 predicted for the old stellar population and associated dust (taken from Misiriotis et al. [38]). It is clear that the prediction (solid line) for the FIR/submm SED falls well short of the observed measurements (symbols).

SEDs. We will use the model of Xilouris et al. [58] to address this question as it is the only model that fits the geometry of stars and dust as seen in the optical, and so should provide the best representation of the intrinsic distributions of the stars and dust in spiral galaxies that can be probed by optical extinction measurements.

To provide a benchmark, we will in the first instance ignore the heating of dust by UV photons, since these could not be included in the analysis of the edge-on systems considered by Xilouris et al. For the FIR emission calculation we use the standard dust model of graphite/silicate from Draine & Lee [16] (and with optical constants specified by Laor & Draine [32]). This is consistent with the Milky Way type extinction law derived for these galaxies. The results are shown in Fig. 3. It is clear that the prediction for the FIR/submm SED falls well short of the observed measurements. In terms of luminosity the shortfall is by a factor of 5. This shows that, according to these models, the old stellar population alone cannot account for the dust emission.

Adding the young stellar disk and associated dust

Lets now add the UV emitting stellar population, but keep the amount and distribution of dust the same. This was considered as a new geometrical component in the model of Popescu et al. [46]. The UV emissivity was assumed to be distributed in a thin disk with the same scalelength as the B band disk, but with an assumed scale height of 90 pc, close to that of the Milky Way ([36]). This is smaller than the scale heights for the optically emitting stars and for the dust distribution derived in the model of Xilouris. The spectral distribution of the UV emission was fixed according to the predictions of a population synthesis model, and its amplitude parameterised in terms of a SFR. Now it is easy to raise the level of the predicted FIR emission to the observed level by simply adjusting the SFR. (see Fig. 4).

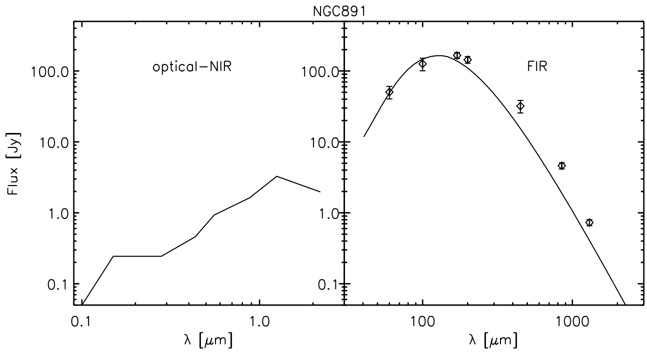

FIGURE 4. The FIR/submm SED of NGC 891 predicted for the old stellar population and associated dust, supplemented by the young stellar disk (taken from Popescu et al. [46]). It is obvious that the model prediction (solid line) for the submm emission falls short of the observed measurements (symbols).

It is obvious from Fig. 4 that the FIR-submm colours are not fitted, in the sense that the model prediction for the submm emission falls short of the observed emission. This suggests either that a further component of dust is present which is not constrained by the optical data, or that the ratio of the submm emissivity to the FIR emissivity is higher than that predicted by the standard Draine & Lee [16] dust model. The latter possibility was recently investigated by Alton et al. [1] and Xilouris [57], who found a submm emissivity enhanced by a factor of 4. This result was obtained by comparing the visual optical depth derived from Xilouris's model with the submm emission, assuming that the same grains emitting in the submm are responsible for the optical extinction. However, this assumption is only true if self-shielding effects of grains are not present. In fact, real galaxies do contain optically thick components, which makes it inevitable that the submm emission will always be higher than predicted on the basis of optical extinction alone. Therefore the solutions obtained by Alton et al. [1] and Xilouris [57] for the submm emissivity can only be treated as upper limits. We should also note that there is no direct observational evidence of enhanced submm emissivity in the *diffuse* ISM. It has only been possible to investigate submm emissivities of grains in discrete clouds, where the brightness of the dust emission from the clouds can be compared with the extinction of background stars. Although enhanced submm emissivities have been found in these investigations, this is not unexpected since the clouds shield the grains from the diffuse UV radiation field, allowing ice mantles to form. Thus, such grains are probably not typical of grains in the bulk of the volume of the galaxy, and, as already noted, are in any case not probed by global extinction studies due to the low filling factor of the clouds. We also note that there are other constraints on the wavelength dependence of grain emissivity (see Li [33]) which would tend to favour a steep decline of emissivity with increasing wavelength in the submm. A steep decline in emissivity would not however lead to the enhanced ratio of the submm to the FIR emissivity needed to explain the FIR/submm colours of galaxies in the absence of a further dust component. In conclusion, there is no independent observational evidence that an interstellar medium composed entirely of *diffuse* dust, as probed by the optical extinction studies, could have

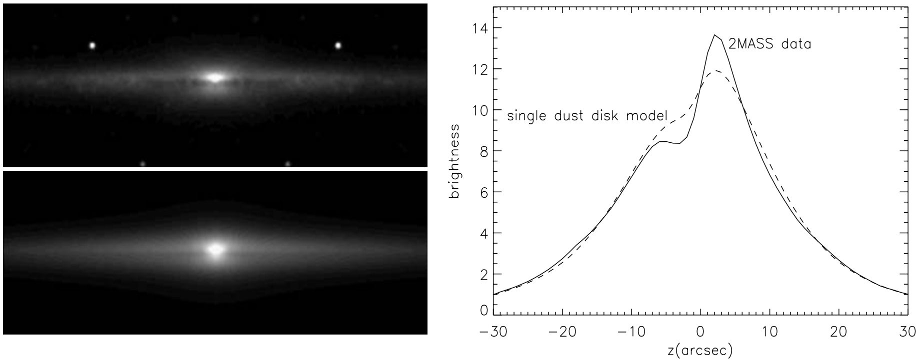

FIGURE 5. Left upper panel: The 2MASS K-band image of NGC 891 (folded). Left lower panel: The simulated K-band image produced using the solution of Xilouris et al. [59], containing a single dust disk associated with the old stellar population. Especially in the central region, the dust lane seen in the 2MASS image is too strong to be accounted for by the single dust disk in this model. This is quantified in the right hand panel, which shows the average brightness of the data and of the model (in arbitrary units) within 50 arcsec of the centre, plotted versus vertical position.

enhanced submm emissivity.

By contrast, there is strong independent observational evidence for a further dust component to explain the observed FIR-submm colours of galaxies. The geometrical model that we presented previously has no dust component associated with the young stellar population, yet we know that such a component exists. We know that dust is associated with the CO emitting layer and we know that this dust is associated with the spiral arms where most of the young stars are formed. The only question is how to prescribe the distribution of this dust. In order to mimic the effect of this component of dust associated with the young stellar population, and in the absence of direct observational constraints, Popescu et al. [46] introduced a second dust disk, having the same scale height as the young stellar disk. A second disk of dust associated with the molecular layer was also considered by Bianchi et al. [6] for the modelling of NGC 6946. Of course, in reality the dust distribution is much more complex due to the spiral arm structure and the (at least in part) clumpy nature of the dust associated with the young stellar population. Because of the presence of clumps, some fraction of the additional dust will be subject to strong self-shielding, and will hardly be seen at all even in the K band images. This may be one reason why the dust lanes observed on K-band images of edge-on galaxies are not much more prominent than the dust lanes predicted from the single dust disk model of Xilouris et al. (see the comparison of Dasyra et al. [12]). Nevertheless, the dust lane seen on the K-band images (Fig. 5) is, particularly in the central regions, too strong to be accounted for by the single dust disk model. This provides a hint that the additional dust layer is more concentrated towards the centre of the galaxy, following the distribution of molecular gas. Finally, we note that the prevalence of clumps in the dust associated with the young stellar population may reduce the dust mass required to account for the submm data, since, as we have already mentioned, dust in optically thick clumps may have an enhanced submm emissivity compared to dust in the diffuse inter-clump medium. Thus, the dust

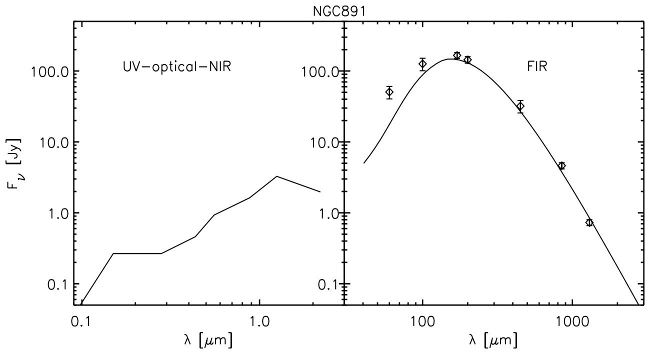

FIGURE 6. The FIR/submm SED of NGC 891 predicted for the old stellar population and associated dust, supplemented by the young stellar disk and associated dust (adapted from Popescu et al. [46]). It is obvious that the model prediction (solid line) for the shorter FIR wavelengths falls short of the observed measurements (symbols), indicating the need for a warmer component of emission.

mass derived by Popescu et al. [46] for the additional dust component should be treated only as an upper limit. In this sense, elements of both the enhanced emissivity hypothesis and the additional dust hypothesis may be needed for a realistic description of the SEDs of normal galaxies.

Despite the complex structure of the dust associated with the young stellar population, the simplification of placing it in a common thin disk with the young stars is a reasonable approximation to predict the optical appearance of galaxies (Misiriotis et al. [39]), as well as the overall energy balance and FIR and submm radial profiles of spiral galaxies (as will be shown here). The effect on the predicted FIR/submm SEDs of including the second disk of dust in the radiative transfer calculation is shown in Fig. 6. Although the longer wavelengths points are now well fitted, the predicted SED is not broad enough to fit the short wavelengths as well. We are clearly missing a warmer component of emission.

Adding the clumpy component of dust with embedded young stars

The lack of a warmer component of emission in the FIR SEDs predicted by the models should not come as a surprise since we have not yet included the localised emission components associated with the star-forming regions. We know that galactic star formation regions have warm dust emission from the local absorption of non-ionising UV produced by the young massive stars. In other words, in addition to the diffuse large scale dust disks, the model must also incorporate a clumpy component of dust, whose spatial distribution is correlated on scales of a few parsecs with the HII regions.

Ideally one would like to have radiation transfer calculations on scales ranging from pc to kpc, to properly understand the propagation of photons on both short and large scales. The closest that has been achieved is the radiative transfer calculation of Sauty et

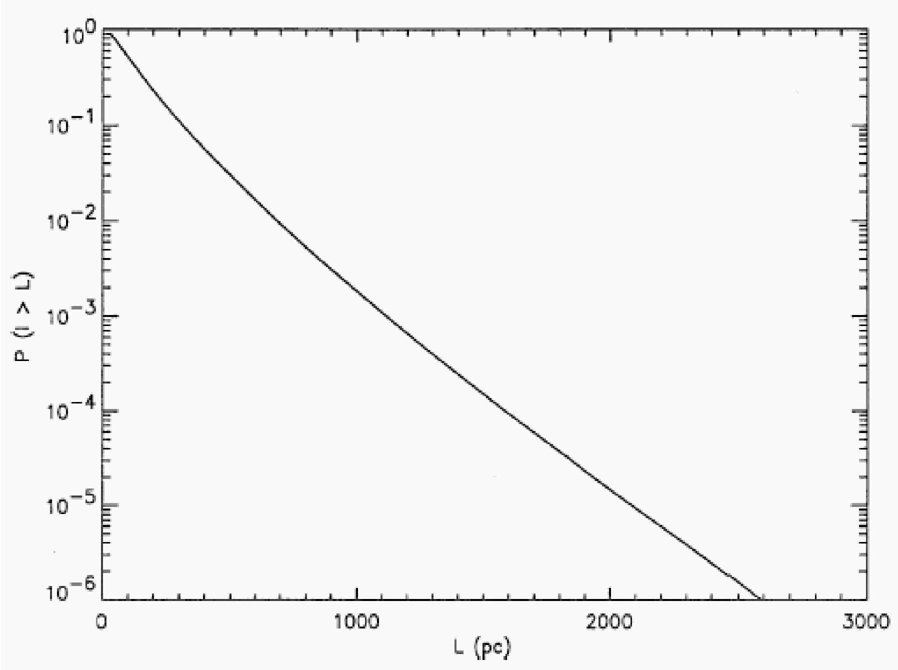

FIGURE 7. Distribution of the distance travelled by UV photons from their parent OB association, before absorption, taken from Sauty et al. [49]. The median distance is 120 pc, and the mean distance is 440 pc.

al. [49]. They calculated the transfer of UV radiation in a interstellar medium consisting of star-forming molecular clouds, visualised at a resolution of 12 pc, as well as a diffuse atomic medium extending up to 12 kpc. They derived the distribution of the distance travelled by UV photons before absorption. Fig. 7 shows that half of the radiation is absorbed within the first $\sim$ 10 resolution elements out to a radius of $\sim$ 120 pc. This calculation cannot tell us, though, what happens within the first cell, which is larger than the size of most HII regions and their immediate surroundings. From an infrared point of view this means that the calculation is not sensitive to the absorption on the shortest scales, and therefore is not sensitive to the warmest grains. It is thus preferable to consider the local absorption and re-emission of UV photons separately from these processes on galactic scales. This approach was adopted both by Silva et al. [50] and by Popescu et al. [46] (see also Charlot & Fall [11]).

The basic idea is to consider that some fraction F of the non-ionising UV is locally absorbed in star-forming complexes and only a fraction $(1-F)$ will go in the diffuse young stellar disk. If this clumpy component is added, the whole FIR/submm SED can indeed be fitted. This can be seen for both the model of Silva et al. [50] in Fig. 8 and for the model of Popescu et al. [46] in Fig. 9. Both figures show the contribution of the diffuse and localised components of the FIR emission. We note that in the model of Silva et al. [50] the diffuse and localised components peak at similar wavelengths,

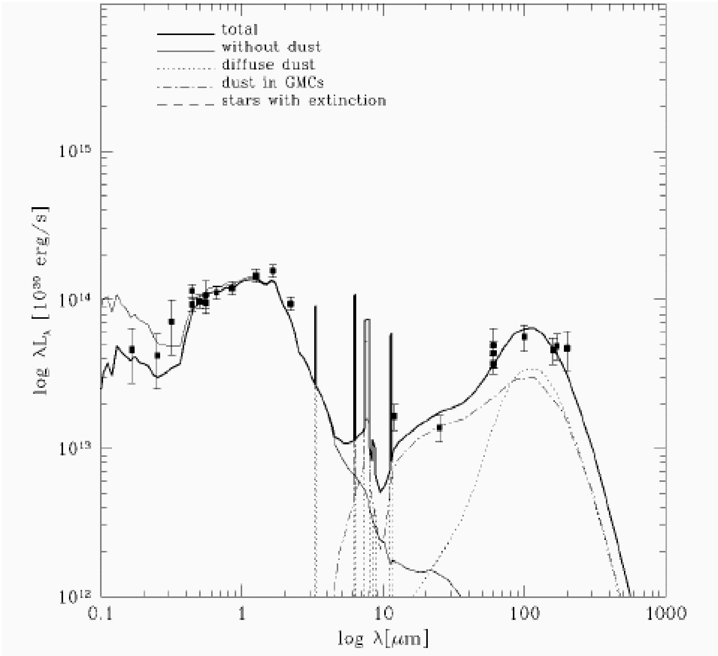

FIGURE 8. Fit to the SED of NGC 6946, taken from Silva et al. [50].

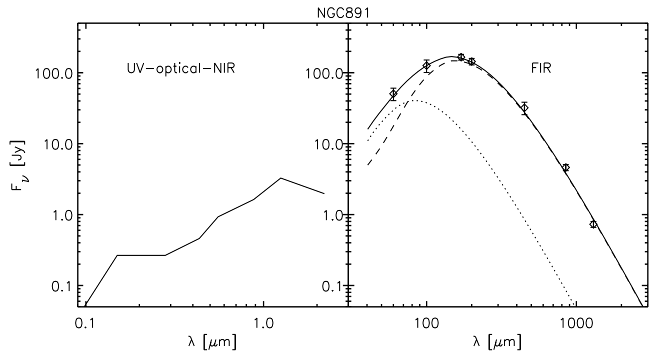

FIGURE 9. The final fit to the FIR/submm SED of NGC 891, taken from Popescu et al. [46]. The total predicted SED is given with the solid line, the diffuse component with the dashed line and the clumpy component with the dotted line. The observed data are given as symbols.

whereas in the model of Popescu et al. [46] they do not. This difference is due to the different treatment of the localised component. The model of Popescu et al. [46] has a fixed empirically determined template for the FIR emission from star-forming complexes, specified by just one parameter (its amplitude - the factor F). The model of Silva et al. [50] incorporates a separate radiative transfer calculation for an idealised star-forming complex, visualised as a molecular cloud with a central embedded source and parameterised by the radius and lifetime of the clouds. Thus, whereas the model of Silva et al. allows for the possible presence of cold dust emission from the optically thick parts of their localised component, the model of Popescu et al. considers only the warm dust emission from this component, and instead includes the cold dust in the second disk of dust which mimics the distribution of molecular material. This conceptual difference will however not have a major effect on the results obtained by the two techniques. The major difference is that one model (Popescu et al.) constrains the geometries of stars and dust from fitting the optical images, and has therefore only a few (in fact just three) free parameters needed to fit the FIR SED, while the other model (Silva et al.) has more free parameters, partly because it also makes a calculation for the photometric evolution of a galaxy, but also because it has to define the geometries with further free parameters.

4.2 Testing the models

We have seen that a realistic model which can predict the observed optical and FIR/submm SEDs needs the following components:

- stellar disk of old stars and associated dust disk
- stellar disk of young stars and associated dust
- bulge of old stars
- clumpy component of dust with embedded young stars

We have also seen that such a model can also predict the optical appearance of galaxies. But a more stringent test of these models is to see if they can also predict the appearance of galaxies in the FIR/submm. Such a test has been done in just one case (for NGC 891; Popescu et al. [47]) by comparing the images at 170 and 200 μm taken with the ISOPHOT instrument on board the Infrared Space Observatory (ISO) with the model predictions of Popescu et al. [46] (see Fig. 10). The comparison between the observed maps and the simulated maps for the diffuse component (at 170 and 200 μm) show a remarkable agreement. To search for small differences between the model and the observations, not detectable in the maps due to the high dynamical range of the displayed data, residual maps of the difference between the observed and the simulated maps are also shown. The residuals show the localised sources, which account for about 10% of the total emission at these wavelengths, in accordance with the prediction of the model. Another comparison is between observed and predicted radial profiles (see Fig. 11, left panel). Here again one can see a very good agreement. Again, the small excess emission in the observed profile is in agreement with the model prediction for localised sources. To date, NGC 891 is the only galaxy for which an intrinsic distribution of dust and stars could be found from a self-consistent modeling and which simultaneously accounts for both the optical and FIR morphologies.

A related test utilising profiles rather than integrated quantities has been done for the radial temperature distribution, namely by comparing that predicted by the model of Bianchi et al. [6] for NGC 6946 with that observed for the Milky Way (see Fig. 11, right panel).

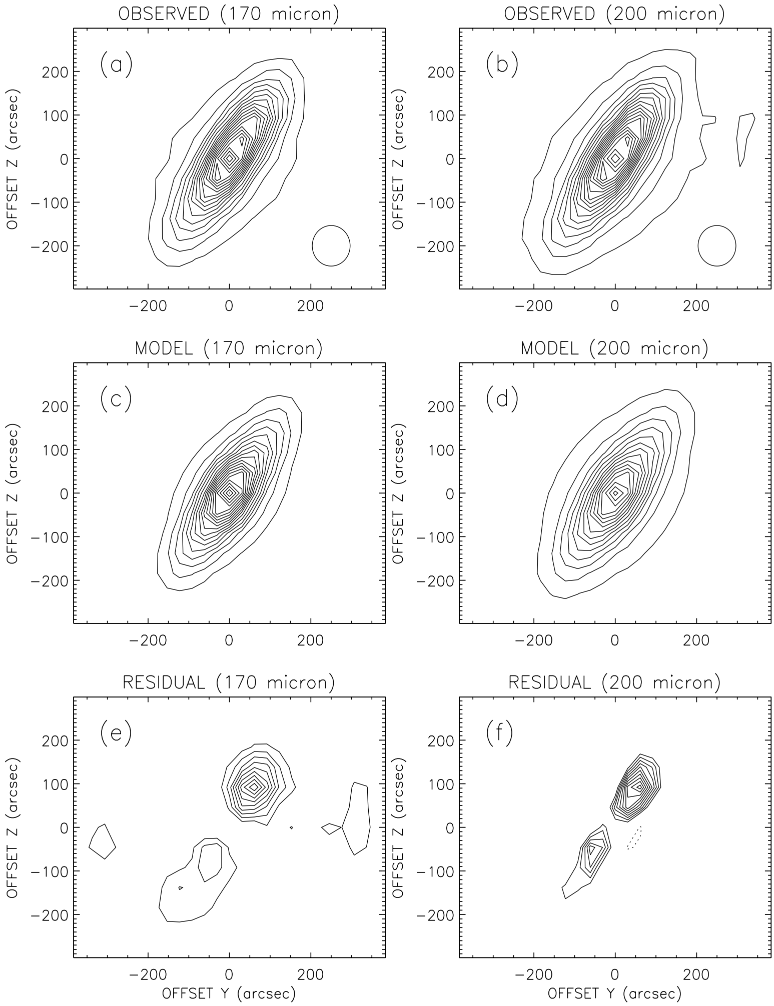

FIGURE 10. Comparison between the observed and predicted FIR maps of NGC 891, taken from Popescu et al. [47]. The top rows show the observed maps taken with the ISOPHOT instrument on board ISO, the middle rows show the predicted maps for the diffuse component, and the bottom rows show the localised sources, obtained as residuals between the observed maps and predicted maps of the diffuse component. The circles from the top rows indicate the footprint (to the FWHM) of the ISOPHOT beam at 170 and 200 μm. Y and Z are the spacecraft coordinates.

It will be desirable to compare predicted and observed FIR/submm maps for a larger number of galaxies. Work in this direction has also been started by Baes et al. [3], this conference.

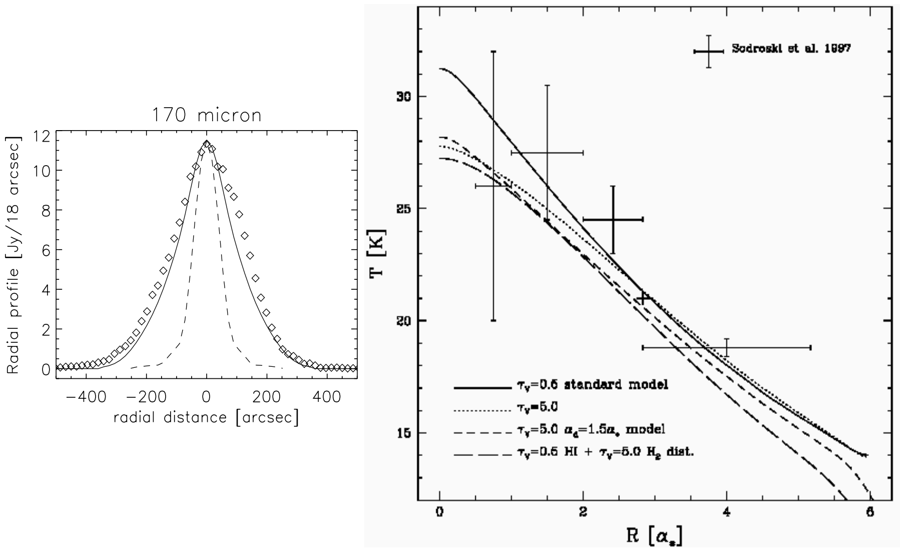

FIGURE 11. Left: Comparison between the observed (symbols) and predicted (solid line) FIR radial profiles of NGC 891, taken from Popescu et al. [47]. The predicted profiles are only for the diffuse component. The small excess emission in the observed profiles is due to localised sources. The observations were done with the ISOPHOT instrument on board ISO. The profiles were obtained by integrating the emission parallel to the minor axis of the galaxy for each bin along the major axis. The sampling of the profiles is 18 arcsec. The dotted lines represent beam profile. Right: Comparison between the predicted radial gradient of temperature in NGC 6946 and the observed one in the Milky Way, taken from Bianchi et al. [6].

4.3 The origin of dust heating

There has been a long standing question in the literature of what is the contribution of different stellar populations to the heating of dust. This question is equivalent to the question of the relative attenuations (averaged over viewing angle) of individual stellar populations, for example in the bulge and in the old and young stellar disks. The self-consistent models of optical/FIR/submm SEDs provide direct means to address this question.

In the modelling of the face-on spiral NGC 6946, Bianchi et al. [6] found that it is the old stellar population that predominantly powers the dust emission, with only 40% of the emission powered by UV photons. However this result assumed that more than 50% of the absorbed UV radiation is channeled directly into the MIR, whereas self-consistent calculations of this percentage show that most of the UV luminosity is actually re-emitted in the FIR. For the same galaxy both Silva et al. [50] and Sauty et al. [49] found that most of the dust heating comes from the young stellar population. In the modelling of the edge-on galaxy NGC 891 Popescu et al. [46] also found that it is the young stellar population that predominantly heats the dust, powering about 70% of the total dust luminosity. Furthermore, because the dust emission from the different components has different characteristic temperatures, one can determine the fractional

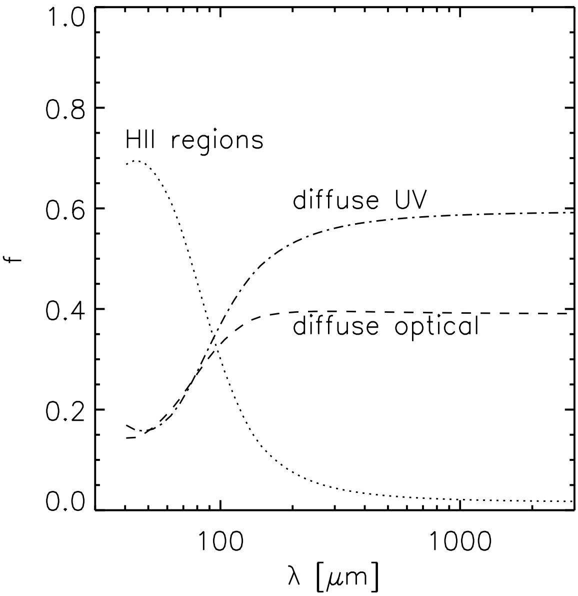

FIGURE 12. The fractional contribution of different stellar components to the dust emission, as a function of FIR/submm wavelength, taken from Popescu et al. [46].

contribution of the different stellar populations as a function of infrared wavelength. For the case of NGC891 (see Fig. 12) one can see that, as expected, HII regions dominate the dust emission at shorter wavelengths. The really interesting feature of this diagram is the predominance of the UV heating in the submm regime. As explained by Tuffs & Popescu [51], this can be understood as follows: the coldest grains are those which are in weaker radiation fields, either in the outer optically thin regions of the disk, or because they are shielded from radiation by optical depth effects. In the first situation the absorption probabilities of photons are controlled by the optical properties of the grains, so the UV photons will dominate the heating. The second situation arises for dust associated with the young stellar population, where the UV emissivity far exceeds the optical emissivity.

4.4 Application to statistical samples

Perhaps the biggest challenge faced by these models is to make them tractable for application to statistical samples of galaxies, while at the same time retaining their fundamental predictive power. A first step in this direction was made by Misiriotis et al. [38] who applied the model of Popescu et al. [46] to further edge-on galaxies modelled in the optical by Xilouris et al. [60]. More recently, Misiriotis et al. [40] used the same model, in simplified form, to fit the FIR SEDs of a submm selected sample of local universe spiral galaxies. As an example of what one can derive from such a study we

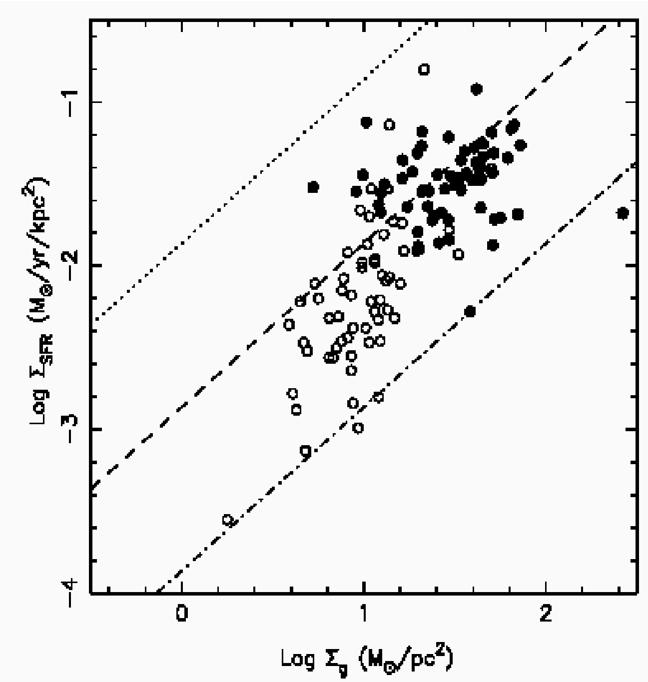

FIGURE 13. Star-formation rate surface density predicted from the SED modelling (solid circles) of a submm selected sample and from the Hα measurements (open circles) of a sample of normal galaxies, as a function of gas surface density (Misiriotis et al. [40]). The dotted, dashed and dot-dashed lines correspond to star formation efficiencies of 100%, 10% and 1% in 10^8 yr.

show the derived star-formation rate surface density as a function of gas surface density (see Fig. 13).

5. A CLOSER LOOK AT THE ROLE OF CLUMPS IN SHAPING THE SEDS OF GALAXIES

We have seen that clumps of dust with embedded young stars are needed to account for the FIR/submm SEDs of normal galaxies. We will refer to such clumps as "active clumps" (with embedded sources). Their main effect is to provide a warm component of emission to the FIR/submm SEDs.

An alternative concept for clumps is to consider them as passive molecular clouds with no embedded stars, such as those introduced by Witt & Gordon [54], or Bianchi et al. [7], and further explored by Witt & Gordon [55] and by Misiriotis & Bianchi [37]. We will refer to such clumps as "passive clumps", since they are randomly distributed with no small scale (of a few pc) correspondence with the young stars. The effect of passive clumps on the FIR/submm SED is exactly the opposite of the effect of the active clumps,

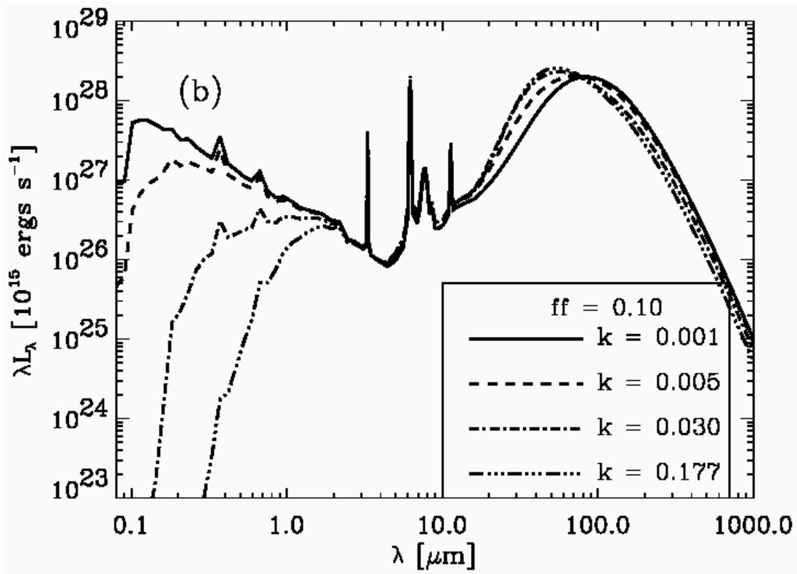

FIGURE 14. The effect of "passive" clumps on the FIR/submm SEDs, taken from Misselt et al. [41]. Model SEDs are for a range of density ratios *k* between the diffuse and clumpy media and for a filling factor ff = 0.1. All models are calculated assuming a spherical shell geometry. It is obvious that the effect of increasing the degree of clumpiness (decreasing k) is to make the SEDs cooler.

namely they provide cooler FIR SEDs. This is illustrated in Fig. 14, which shows results from a calculation made by Misselt et al. [41] for a spherical shell geometry with varying degrees of clumpiness. The reason why the grains are colder when the dust is distributed in passive clumps is simply that light is no longer reaching grains in the body of the clumps. Of course this effect only occurs when the clumps are optically thick. A medium of optically thin clumps would make no measurable difference to the FIR SED compared to the same dust homogeneously distributed.

The effect of the clumps on the UV/optical/NIR SEDs is also dependent on whether the clumps are "active" or "passive". The effect of "active" clumps on the attenuation characteristics of spiral galaxies has been studied by Bianchi et al. [7], Misiriotis & Bianchi [37] and Tuffs et al. [53]. Their effect has been also considered by Charlot & Fall [11] and, in the context of starburst galaxies, by Dopita et al. [15]. Unlike the effect of diffuse dust in a disk galaxy, the attenuation produced by "active" clumps does not strongly depend on the inclination of the galaxy. Furthermore, the wavelength dependence of the attenuation is no longer primarily determined by the optical properties of the grains, but instead by the different blocking action of the clumps on the photons emitted by stars of different ages, and thus masses. This effect arises because longer lived stars are typically to be found at larger distances from their parent molecular clouds. Furthermore, the introduction of dust in the form of active clumps will increase the global attenuation of a galaxy more than if the same dust had been added to the diffuse interstellar medium. This can be physically attributed to the placing of the clumps in the direct vicinity of the UV emitting stars.

The effect of “passive” clumps on the attenuation characteristics of spiral galaxies has been studied by Bianchi et al. [7], Kuchinski et al. [28], Misiriotis & Bianchi [37] and Pierini et al. [42]. Their main effect is to lower the global attenuation of the galaxy and only to a lesser degree to change the dependence of attenuation on wavelength. Details of the dependence of the attenuation on inclination and wavelength appear to depend strongly on the parameterisation of the clumps, for example whether the clumps have a fixed density or have a fixed density contrast to the diffuse medium (see Bianchi et al. [5]).

In summary, the major effects of clumps on SEDs are as follows:

- “active” clumps (with embedded sources)
  - tend to make the FIR/submm colours warmer
  - tend to increase the attenuation of the UV/optical emission
- “passive” clumps
  - tend to make the FIR/submm colours cooler
  - tend to decrease the attenuation of the UV/optical emission

In practice, the description of real galaxies requires the presence of both “passive” and “active” clumps. Indeed, the same physical interstellar cloud can act either as a passive or an active clump, depending on the observed wavelength. For example, molecular clouds will behave as “active” clumps in the UV, due to their strong spatial correlation with young stars, and as “passive” clumps in the optical/NIR, due to the smooth distribution of the old stellar population. This has an interesting consequence on the slope of the attenuation curve of spiral galaxies, namely that they will be steeper than predicted by homogeneous models. This may be important to bear in mind when considering the contribution of spiral galaxies to the Madau’s plot. In the dust emission, clumps with embedded sources provide the short wavelength luminosity. Passive clumps are unimportant in terms of luminosity, but will increase the amplitude of the submm emission deep in the Rayleigh-Jeans regime.

Of course the results we have described are for a particularly simple situation, that of a two phase medium (diffuse and clumps). In reality the interstellar medium is turbulent, presenting a whole distribution of column densities along different lines of sight. The effect of this more realistic structure on attenuation has been considered by Fischera et al. [21], Fischera & Dopita [19], [20].

6. MODELLING THE ATTENUATION OF STELLAR LIGHT IN GALAXIES

Traditionally, the effect of dust in attenuating stellar light in galaxies has been quantified purely empirically by statistical analysis of the variation of optical surface brightness with inclination. However, this variation is small in comparison with the scatter, so that this method is not useful for estimating the attenuation of light in individual galaxies. For this reason, there has always been a strong incentive to develop models for the attenuation of stellar light in galaxies. With the development of radiative transfer calculations on high speed computers, such models have become a practical possibility. The problem, however, has been to identify realistic geometries for stars and dust, since, as demonstrated in this review, these are not well constrained by optical data alone. Consequently, until very recently, models for attenuation have largely concentrated on evaluating the effect different choices for the geometries of stars and dust would have on the attenuation. The geometry was varied to investigate the effect of the inclusion or non-inclusion of different structures, such as clumps or bulges, as well as simply to investigate the effects of varying the parameters of structures, such as scalelengths and scaleheights of disks of dust and stars.

This type of work was done by Bianchi [8], Ferrara et al. [18], Baes & Dejonghe [2] and Pierini et al. [42]. For example Ferrara et al. provided an atlas of dust attenuation calculated as a function of geometry, inclination, dust optical depth, and extinction properties. This atlas is available in electronic format. As an application they compared the predicted variation of apparent magnitude with inclination with the observed one. Pierini et al. [42] investigated the effect of the dust being distributed in "passive" clumps (as defined in Sect. 5), rather than homogeneously. In this work the large scale distributions of stars and dust and the dust-type were fixed, and the attenuation characteristics of the bulge and disk as seen through the whole distribution of dust were calculated separately.

The recent development of models which reproduce the observed optical/FIR/submm SEDs and the surface brightness distributions in both optical and FIR range means that the geometry of stars and dust is no longer a free choice, but should conform to the solution adopted by these models. Such an approach was taken by Tuffs et al. [53], who used the SED model of Popescu et al. [46] to calculate the attenuation of stellar light in spiral galaxies. Unlike previous studies of attenuation, this model incorporates a second disk of dust and "active" clumps. These new elements affect both the inclination and wavelength dependence of attenuation. In order to make the model applicable to a wide range of bulge-to-disk ratios and degrees of clumpiness, separate calculations were done for the main stellar components: older stellar disk, young stellar disk and bulge, each seen through two dust disks, while the clumpy component was treated analytically. In Fig. 15 we show examples of attenuation curves taken from Tuffs et al. [53]. For all geometrical components there is an obvious increase in attenuation with increasing inclination, with the exception of the attenuation of the bulge when the inclination approaches the edge-on view. Also, the increase in attenuation with increasing inclination is stronger for larger face-on opacities than for lower ones, irrespective of geometry or wavelength. These solutions of attenuation as a function of inclination, opacity and wavelength are available in electronic format for general use by the community. These data can be used to construct attenuation curves for any combination of bulge-to-disk ratio and clumpiness factor. The effect of varying the bulge-to-disk ratio is one of the most important factors in shaping the attenuation curves in the optical/NIR range. In general, ignoring the presence of bulges can lead to a systematic overestimate of the opacity of disks. Also the effect of varying the clumpiness factor is one of the most important factors in shaping the attenuation curves in the UV range.

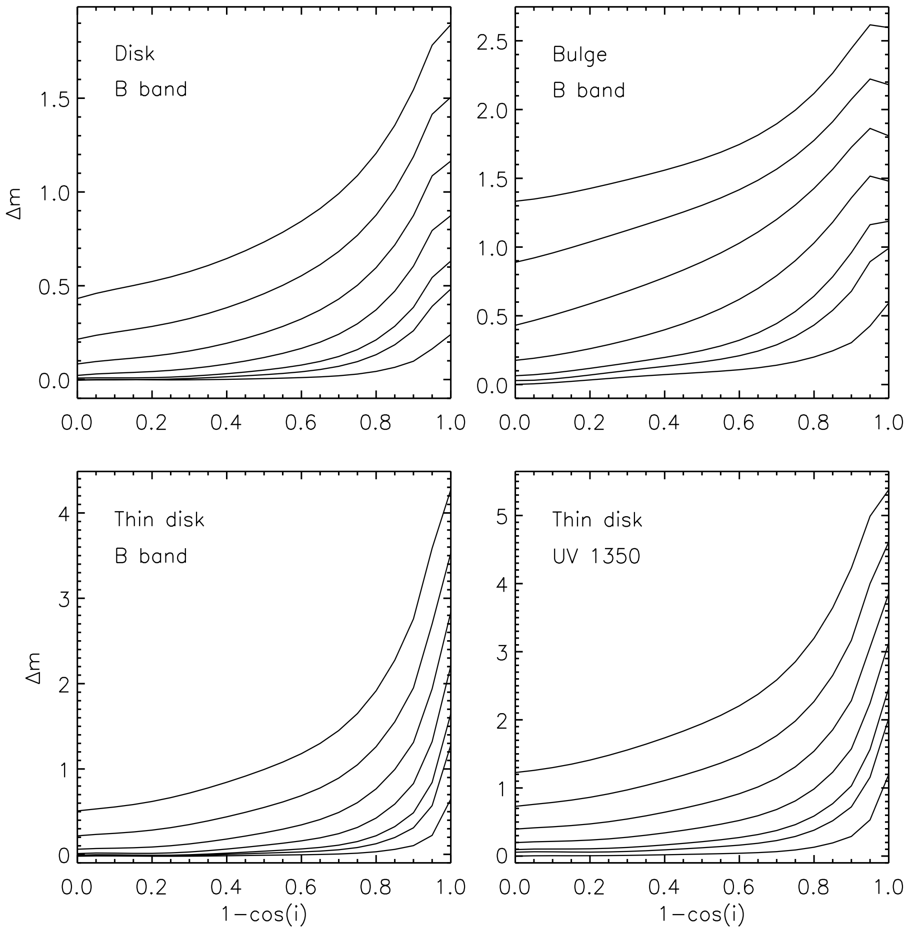

FIGURE 15. Examples taken from Tuffs et al. [53] of the dependence of attenuation (Δm) on inclination (i) for the main stellar components their model: disk (top left), bulge(top right), and thin disk (bottom left and right). The examples are plotted for the B band for the disk and bulge, and both for the B band and UV 1350 for the thin disk. Each panel shows (from top to bottom) 7 attenuation curves, corresponding to central face-on B band optical depths of τ^f_B: 8, 4, 2, 1, 0.5, 0.3, and 0.1. The face-on orientation corresponds to $1-\cos(i) = 0.0$ and the edge-on orientation corresponds to $1-\cos(i) = 1.0$.

OUTLOOK

Although much has already been achieved, there are clear objectives that need to be met to make further progress in this field. First of all, there is still the need to make detailed modelling of nearby face-on galaxies, both in terms of their integrated SEDs and surface-brightness distributions. Unlike the edge-on geometry, the face-on view also allows the young stellar population and associated dust to be constrained by the morphology of the extincted disk in the UV. Secondly, as already mentioned, we must make the models tractable for application to statistical samples of galaxies, while at the same time retaining their fundamental predictive power. For example, from the perspective of the infrared community, we must provide a viable alternative to Planck curves.

Finally, one would like to impose a physically self-consistent framework on these models, in which the geometry of the stellar populations and of the gas and dust is calculated self-consistently in terms of the gravitational potential of the galaxy.

ACKNOWLEDGMENTS

We would like to thank N.D. Kylafis, M.A. Dopita, A. Misiriotis, M. Xilouris, J. Fischera, B.F. Madore & H.J. Völk for the many discussions and fruitful collaboration we have enjoyed over the last years, without which this paper would not have been possible. N.D. Kylafis is also acknowledged for a critical reading of this manuscript.

REFERENCES

1. Alton, P.B., Xilouris, E.M., Misiriotis, A., Dasyra, K.M., & Dumke, M. 2004, A&A 425, 109
2. Baes, M. & Dejonghe, H. 2001, MNRAS 326, 733
3. Baes, M., Dejonghe, H. & Davies, J.I. 2005, in "The Spectral Energy Distribution of Gas-Rich Galaxies: Confronting Models with Data", Heidelberg, 4-8 Oct. 2004, eds. C.C. Popescu & R.J. Tuffs, AIP Conf. Ser., in press
4. Buat, V. & Xu, C. 1996, A&A 306, 61
5. Bianchi, S. 2004, in Astrophysics of Dust, Proceedings of the conference held 26-30 May, 2003 at Estes Park, Colorado, USA. eds. A.N. Witt, G.C. Clayton and B.T. Draine. ASP Conference Proceedings, Vol. 309. San Francisco: Astronomical Society of the Pacific, p. 771
6. Bianchi, S., Davies, J.I., & Alton, P.B. 2000a, A&A, 359, 65
7. Bianchi, S., Ferrara, A., Davies, J.I., & Alton, P.B. 2000b, MNRAS 311, 601
8. Bianchi, S., Ferrara, A. & Giovanardi, C. 1996, ApJ 465, 127
9. Calzetti, D. 2001a, PASP 113, 1449
10. Calzetti, D. 2001b, New Astronomy Reviews 45, 601
11. Charlot, S. & Fall, S.M. 2000, ApJ 539, 718
12. Dasyra, K.M., Xilouris, E.M., Misiriotis, A., & Kylafis, N.D. 2005, A&A submitted
13. Disney, M., Davies, J., Phillipps, S. 1989, MNRAS 239, 939
15. Dopita, M.A. 2005, in "The Spectral Energy Distribution of Gas-Rich Galaxies: Confronting Models with Data", Heidelberg, 4-8 Oct. 2004, eds. C.C. Popescu & R.J. Tuffs, AIP Conf. Ser., in press
15. Dopita, M.A., Groves, B.A., Fischera, J., Sutherland, R.S., Tuffs, R.J. et al. 2005, ApJ, in press
16. Draine B.T. & Lee H.M. 1984, ApJ, 285, 89
17. Dwek, E. 2005, in "The Spectral Energy Distribution of Gas-Rich Galaxies: Confronting Models with Data", Heidelberg, 4-8 Oct. 2004, eds. C.C. Popescu & R.J. Tuffs, AIP Conf. Ser., in press
18. Ferrara, A., Bianchi, S., Cimatti, A., & Giovanardi, C. 1999, ApJS 123, 437
19. Fischera, J., & Dopita, M.A. 2004, ApJ 611, 919
20. Fischera, J., & Dopita, M.A. 2005, ApJ in press
21. Fischera, J., Dopita, M.A. & Sutherland, R.S. 2003, ApJ 599, L21
22. Galliano, F., Madden, S.C., Jones, A.P., Wilson, C.D., Bernard, J.-P., et al. 2003, A&A 407, 159
23. Gordon, K. 2005, in "The Spectral Energy Distribution of Gas-Rich Galaxies: Confronting Models with Data", Heidelberg, 4-8 Oct. 2004, eds. C.C. Popescu & R.J. Tuffs, AIP Conf. Ser., in press
24. Gordon, K.D., Misselt, K.A., Witt, A.N., & Clayton, G.C. 2001, ApJ 551, 269
25. Granato, G.L., Lacey, C.G., Silva, L., Bressan, A., Baugh, C.M., Cole, S. & Frenk, C.S., 2000, ApJ 542, 710
26. Guhathakurta P., & Draine B.T. 1989, ApJ, 345, 230

27. Kewley, L.J., Geller, M.J. & Jansen, R.A. 2005, in "The Spectral Energy Distribution of Gas-Rich Galaxies: Confronting Models with Data", Heidelberg, 4-8 Oct. 2004, eds. C.C. Popescu & R.J. Tuffs, AIP Conf. Ser., in press
28. Kuchinski, L.E., Terndrup, D.M., Gordon, K.D., Witt, A.N. 1998, AJ, 115, 1438
29. Kylafis N.D. & Bahcall J.N., 1987, ApJ 317, 637
30. Kylafis, N. & Misiriotis, A. 2005, in "The many scales in the Universe - JENAM 2004 Astrophysics Reviews", Granada, Spain, September 13-17, 2004, eds. Jose Carlos del Toro Iniesta et al., Kluwer Academic Publishers, in press
31. Kylafis, N.D. & Xilouris, E.M. 2005, in "The Spectral Energy Distribution of Gas-Rich Galaxies: Confronting Models with Data", Heidelberg, 4-8 Oct. 2004, eds. C.C. Popescu & R.J. Tuffs, AIP Conf. Ser., in press
32. Laor A., & Draine B.T. 1993, ApJ 402, 441
33. Li, A. 2005, in "The Spectral Energy Distribution of Gas-Rich Galaxies: Confronting Models with Data", Heidelberg, 4-8 Oct. 2004, eds. C.C. Popescu & R.J. Tuffs, AIP Conf. Ser., in press
34. Leitherer, C. 2005, in "The Spectral Energy Distribution of Gas-Rich Galaxies: Confronting Models with Data", Heidelberg, 4-8 Oct. 2004, eds. C.C. Popescu & R.J. Tuffs, AIP Conf. Ser., in press
35. Matthews, L.D., & Wood, K. 2001, ApJ 548, 150
36. Mihalas D., Binney J., 1981, Galactic astronomy: Structure and kinematics (San Francisco, CA, W.H. Freeman and Co.)
37. Misiriotis A. & Bianchi, S. 2002, A&A 384, 866
38. Misiriotis A., Popescu, C.C., Tuffs, R.J., & Kylafis, N.D. 2001, A&A, 372, 775
39. Misiriotis A., Kylafis, N.D., Papamstorakis, J., & Xilouris, E.M. 2002, A&A 353, 117
40. Misiriotis, A., Papadakis, I.E., Kylafis, N.D., & Papamastorakis, J. 2004, A&A, 417 39
41. Misselt, K.A., Gordon, K.D., Clayton, G.C., & Wolff, M.J. 2001, ApJ 551, 277
42. Pierini, D., Gordon, K.D., Witt, A.N., Madsen, G.J. 2004, ApJ 617, 1022
43. Piovan, L., Tantalo, R. & Chiosi, C. 2005, in "The Spectral Energy Distribution of Gas-Rich Galaxies: Confronting Models with Data", Heidelberg, 4-8 Oct. 2004, eds. C.C. Popescu & R.J. Tuffs, AIP Conf. Ser., in press
44. Popescu, C.C., Tuffs, R.J. 2002, Reviews in Modern Astronomy, vol 15., Edited by Reinhard E. Schielicke. Wiley, ISBN 352640404X, p.239
45. Popescu, C.C. & Tuffs, R.J. 2003, A&A 410, L21
46. Popescu, C.C., Misiriotis A., Kylafis, N.D., Tuffs, R.J., & Fischera, J., 2000, A&A, 362, 138
47. Popescu, C.C., Tuffs, R.J., Kylafis, N.D. & Madore, B.F. 2004, A&A 414, 45
48. Rocca-Volmerange, B. 2005, in "The Spectral Energy Distribution of Gas-Rich Galaxies: Confronting Models with Data", Heidelberg, 4-8 Oct. 2004, eds. C.C. Popescu & R.J. Tuffs, AIP Conf. Ser., in press
49. Sauty, S., Gerin, M., & Casoli, F. 1998, A&A 339, 19
50. Silva, L., Granato, G.L., Bressan, A., Danese, L. 1998, ApJ 509, 103
51. Tuffs, R.J. & Popescu, C.C. 2003, in "Exploiting the ISO Data Archive. Infrared Astronomy in the Internet Age", Siguenza, Spain 24-27 June, 2002. Eds. C. Gry et al., ESA SP-511, p. 239.
52. Tuffs, R.J. & Popescu, C.C. 2005, in "The Spectral Energy Distribution of Gas-Rich Galaxies: Confronting Models with Data", Heidelberg, 4-8 Oct. 2004, eds. C.C. Popescu & R.J. Tuffs, AIP Conf. Ser., in press
53. Tuffs, R.J., Popescu, C.C., Völk, H.J., Kylafis, N.D., & Dopita, M.A. 2004, A&A 419, 821
54. Witt, A.N., & Gordon, K.D. 1996, ApJ 463, 681
55. Witt, A.N., & Gordon, K.D. 2000, ApJ 528, 799
56. Witt, A.N., Thronson, H.A. & Capuano, J.M. 1992, ApJ 393, 611
57. Xilouris, E.M. 2005, in "The Spectral Energy Distribution of Gas-Rich Galaxies: Confronting Models with Data", Heidelberg, 4-8 Oct. 2004, eds. C.C. Popescu & R.J. Tuffs, AIP Conf. Ser., in press
58. Xilouris, E.M., Kylafis, N.D., Papamastorakis, J., Paleologou E.V. & Haerendel, G. 1997, A&A, 325, 135
59. Xilouris, E.M., Alton, P.B., Davies, J.I., et al., 1998, A&A, 331, 894
60. Xilouris, E.M., Byun, Y.I., Kylafis, N.D., Paleologou, E.V., Papamastorakis, J., 1999, A&A, 344, 868
61. Xu, C. & Buat, V. 1995, A&A 293, L65
62. Xu, C. & Helou, G. 1996, ApJ 456, 163
63. Xu, C., Buat, V., Boselli, A. & Gavazzi, G. 1997, A&A 324, 32